Case Study: Dynamic Performance Enhancement of Power Substation Reactor Foundations through Vibration Analysis and Self-Leveling Concrete Retrofitting

Sangeeta Pandey
Department of Civil Engineering, National Institute of Technology, Patna, India
sangeetap.ph21.ce@nitp.ac.in (corresponding author)

Ajay Kumar Sinha
Department of Civil Engineering, National Institute of Technology, Patna, India
aksinha@nitp.ac.in

Received: 23 January 2026 | Revised: 7 February 2026 and 19 February 2026 | Accepted: 20 February 2026

 DOI: https://doi.org/10.48084/etasr.17725

ABSTRACT

This study proposes a systematic methodology for seismic retrofitting of vibration-sensitive reactor foundations in high-voltage power substations. Structural distress in 80 MVAR bus reactor foundations—marked by surface unevenness and 3–4 mm wide, 500–650 mm deep cracks concentrated at steel–concrete interfaces—was identified through comprehensive diagnostics including visual inspection, concrete core testing, carbonation assessment, and vibration heat-map analysis. Although concrete strength (28.64 N/mm²) and reinforcement conditions were found satisfactory, vibration mapping revealed pronounced dynamic instability and localized stiffness loss. Considering the operational constraints of a continuously energized substation, a phased retrofitting strategy was implemented using self-leveling concrete, micro-concreting, and pressurized epoxy injection grouting, selected for their superior flowability, bonding efficiency, shrinkage control, and vibration-damping characteristics. Heat-map-guided rehabilitation allowed precise treatment of critical stress zones. Post-retrofitting evaluations exhibited significant improvement, with average vibration decreasing from 23.25 µm to 4.98 µm and peak displacement reducing to 23.31 µm, indicating restored monolithic behavior and enhanced structural stiffness. The proposed framework strengthens the seismic and dynamic performance of reactor foundations, improving the resilience and long-term operational reliability of critical power-substation infrastructure.

Keywords-case study; heat map analysis; self-leveling concrete; reactor foundation

I. INTRODUCTION

Power stations because they play a significant role in maintaining grid stability during normal operations and emergencies. Among the key components in high-voltage substations is the bus reactor, which regulates voltage levels by absorbing reactive power. Other equipment foundations in power substations exhibit dynamic responses only when their respective machines operate; however, reactor foundations are continuously exposed to magnetostriction-induced vibratory forces, making them more susceptible to long-term dynamic distress. These reactors are supported on Reinforced Cement Concrete (RCC) foundations of M20 grade in general. Each foundation is configured either as a pedestal or a raft foundation. The foundations are designed to withstand multiple load conditions, including electromagnetic forces, thermal expansion, static loads, and dynamic vibration impacts [1]. To ensure operational reliability and structural integrity under dynamic and seismic loads, the foundations are equipped with anchor bolt assemblies for secure fixation, vibration-damping provisions to mitigate reactor-induced oscillations, and integrated grounding systems for effective fault current dissipation [2]. Despite these provisions, structural distress was observed in several reactor foundations at a major substation. Unevenness of surface and cracks measuring 3–4 mm in width and extending 500–650 mm in depth were detected primarily at the steel–concrete interface during inspections. Such defects pose significant risks to power system continuity, necessitating immediate remedial action [3].

As machine foundations are subjected to reactor-induced vibrations, these reinforced concrete blocks must ensure both seismic resilience and structural integrity. Comprehensive visual inspections, along with non-destructive tests [4], core

sampling [5], and carbonation analysis [6], confirmed that the concrete and embedded reinforcement were in acceptable condition. Vibration heat maps [7] showed that while reactor vibrations remained within acceptable limits, the vibrations transmitted to the foundation exceeded permissible thresholds. Consequently, cracks developed primarily at the steel–concrete interface, indicating repairable damage driven by surface unevenness. Because a substation shutdown was not feasible, a phased retrofitting strategy was implemented. The method incorporated self-leveling concrete [8, 9], micro-concreting [10], and epoxy injection grouting [11-13], selected for their flowability, thermal compatibility, energy dissipation, and bonding efficiency. Self-leveling concrete improved surface uniformity and load transfer, and post-retrofitting heat-map evaluations confirmed significant enhancement in structural integrity and dynamic performance.

This study contributes a novel integrated diagnostic and retrofitting framework for vibration-sensitive reactor foundations. The novelty lies in (i) combining vibration heat-map analytics with Non-Destructive Testing (NDT) to identify stiffness-loss zones, (ii) executing a data-driven retrofit under live substation conditions, (iii) employing a synergistic system of self-leveling concrete, micro-concrete, and epoxy injection tailored for vibration damping, and (iv) demonstrating significant dynamic improvement with displacement reducing from 23.25 µm to 4.98 µm. This establishes a replicable methodology for seismic and dynamic rehabilitation of critical substation infrastructure.

A. Problem Identification

The 80MVAR reactor foundations exhibited significant cracking, presenting important operational and structural safety concerns for the substation and associated transmission infrastructure. More specifically, the foundations exhibited a top uneven surface and crack formation. Most cracks were concentrated at the structural steel–concrete interface (Figures 1 and 2). Field measurements revealed that cracks demonstrated widths ranging from 3 to 4 mm and penetration depths between 500 mm and 650 mm. Diagnostics showed that the reactor-induced vibrations and localized stress concentrations caused surface unevenness, initiating cracks and driving their progressive propagation.

Fig. 1. Reactor foundation, front view with cracks.

Fig. 2. Reactor foundation, back view with cracks.

II. INVESTIGATIVE MEASURES TAKEN

A. Physical Test

To evaluate the compressive strength of the foundation core, samples were extracted (Figure 3) from randomly selected locations while avoiding reinforcement zones to ensure reliable sampling (Table I). The results confirmed that concrete quality remained satisfactory (Figure 4, Table II), indicating adequate structural integrity. All testing procedures adhered to [5].

Fig. 3. Core extraction.

TABLE I. CORE SPECIFICATION

Mark	Weight of specimen (gm)	Dia (mm)	Height (mm)	Height/ diameter ratio	Correction factor (A)	Appearance of fractured face
1	931	68.12	85.09	1.25	0.93	Satisfactory
2	813	68.2	115.6	1.69	0.95	Satisfactory
3	934	68.5	91.54	1.34	0.99	Satisfactory

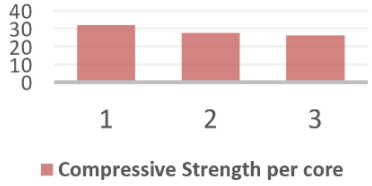

Fig. 4. Compressive strength/core.

TABLE II. CORE TEST RESULT

Core no.	Cross-sectional area (B) (mm²)	Observed load (C) (KN)	Corrected load (C) (KN)	Comp. strength (E) (N/mm²)	Corr. strength (F) (N/mm²)	Corr. comp. strength (G) (N/mm²)	Equivalent cube comp. strength (N/mm²) (1.12)
1	3642	112.2	112.2	30.8	28.64	28.64	32.07
2	3657	95.2	95.2	26.03	24.73	24.73	27.7
3	3689	87.2	87.2	23.6	23.36	23.36	26.16

B. Chemical Test

Carbonation testing was conducted to assess the corrosion status of reinforcement in cracked reactor foundations. In accordance with [6], no carbonation effect was observed, confirming the absence of corrosion risk.

C. Vibration Analysis

The vibration characteristics of the reactor foundation were evaluated to verify compliance with applicable standards. A grid-based analysis was performed to map displacement patterns and identify stress-prone zones. For accurate spatial interpretation, the heat map was superimposed onto the 4.8×4.2 m foundation layout, divided into 40 (5×8) segments, with displacement considered up to 90 µm. This enabled correlation of vibration hotspots with physical locations such as rail anchorage and steel–concrete interfaces (Figure 5).

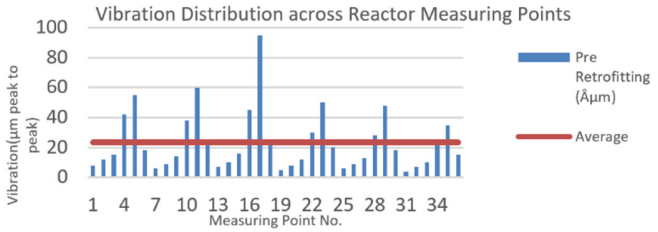

Fig. 5. Vibration distribution across the reactor.

The heat map analysis revealed distinct vibration hotspots, highlighted in bright yellow and orange, located near coordinates (4,2), (4,1), and (3,1.5). These regions corresponded to critical stress zones, mainly at rail anchorage points and steel–concrete interface connections, which are inherently susceptible to dynamic loading. Conversely, darker regions indicated minimal vibration activity, signifying areas of structural stability (Figures 6 and 7).

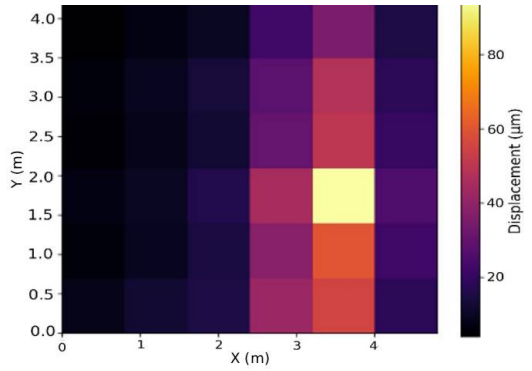

Fig. 6. Heat map pre-retrofitting.

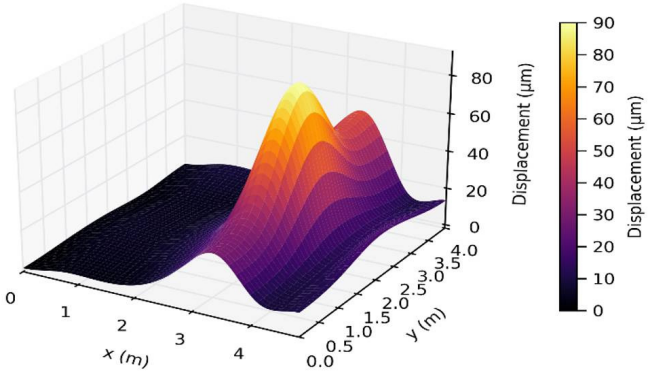

Fig. 7. Three-dimensional view pre-retrofitting.

The observed crack propagation patterns exhibited strong correlation with these high-vibration zones, confirming that the steel–concrete interface represents the most vulnerable region under operational and seismic-induced dynamic stresses. This finding aligns with the requirements of [7], wherein the recorded average displacement exceeded acceptable limits, necessitating remedial measures to restore structural integrity.

III. TECHNICAL CORRELATION OF HEAT MAPS WITH RCC FOUNDATION BEHAVIOR

The vibration heat maps generated for reactor foundations serve as a diagnostic tool to identify zones of dynamic stress concentration and stiffness degradation within the RCC foundation. Bright regions in the heat map correspond to high vibration amplitudes near steel–concrete interfaces and rail anchorage points, indicating localized loss of rigidity and uneven load transfer. This phenomenon can be explained using the fundamental vibration response equation:

$$\delta = \frac{F_d}{k} \quad (1)$$

where , δ =displacement amplitude (µm), F_d =dynamic force induced by reactor operation (N), k =stiffness of the RCC foundation (N/mm).

The dynamic force is further expressed as:

$$F_d = m \cdot a = m \cdot (2\pi f)^2 \cdot \delta \quad (2)$$

where m=reactor mass (kg), f=vibration frequency (Hz). High δ values observed in heat map hotspots imply either reduced stiffness k or increased dynamic excitation F_d, both of which accelerate unevenness of the surface, crack propagation, and interface debonding. Pre-retrofitting analysis revealed an average displacement of 23.25 µm and a peak of 95 µm, exceeding ISO 10816-3 limits, confirming structural vulnerability.

IV. PROPOSED SOLUTION

Self-leveling concreting, micro-concreting, and epoxy grouting form an advanced retrofitting system for vibration-sensitive foundations.

A. Self-Leveling Concrete

Self-leveling concrete is a high-flow, non-shrink material that creates a smooth, level surface without vibration or manual compaction. It spreads under gravity, filling voids and eliminating unevenness that causes dynamic stress. Its formulation ensures uniformity, shrinkage compensation, and high early strength without chlorides, providing excellent bonding with load-bearing areas. In reactor foundations, a 25 mm layer was applied above RCC to achieve precise leveling, improve load transfer, and enhance vibration damping, significantly reducing dynamic amplification and extending service life. The properties of self-leveling concrete are illustrated in Table III.

TABLE III. PROPERTIES OF SELF-LEVELING CONCRETE

Tensile strength	3.5 N/mm^2 @ 28 days			
Pullout bond strength	17N/mm^2 @ 7 days, 20N/mm^2 @ 28 days			
Coefficient of thermal expansion	11×10^{-6}/ºC			
Pressure to restrain	0.004 N/mm^2 approx.			
Grout consistency	Max. flow distance in mm			
	Gap width (mm)	50mm head	100mm head	250mm head
Flowability	30	350	1000	1500
	40	500	1500	2000
	50	900	2000	3000

B. Micro Concreting

Micro-concrete is a high-strength, shrinkage-compensated material that fills fine gaps and inaccessible voids. It offers thermal compatibility, capillary absorption resistance, and superior flexural strength, ensuring stiffness and durability for structural rehabilitation in critical infrastructure applications. Its properties are detailed in Table IV.

TABLE IV. PROPERTIES OF MICRO-CONCRETE

Ambient air temperature	+5°C min./+40°C max.	
Consumption	1900 kg of powder per m^3 of concrete	
Mixing ratio	Water:Powder = 0.14 to 0.16 (by weight)	
Splitting tensile strength	≥3.5 N/mm^2 (water:powder = 0.15, 28 days, +30°C)	
Expansion	Up to 4%	
Compressive strength	Curing time	Compressive strength
	7 days	≥45 N/mm^2
	8 days	≥65 N/mm^2

C. Epoxy Grout

Epoxy grout is a high-strength, non-shrink material with superior adhesion, flexibility, and toughness. It effectively absorbs and dissipates dynamic loads, making it ideal for sealing deep cracks and restoring structural continuity in vibration-sensitive foundations. Its properties are outlined in Table V.

TABLE V. PROPERTIES OF EPOXY GROUT

Tensile strength in flexure	≥30 N/mm^2 (10 days/+30°C)
Shrinkage	Hardens without shrinkage
Tensile adhesion strength	≥10 N/mm^2 (dry)(14 days/+30°C)
Consumption	0.3-0.8 kg/m^2, as per substrate condition
Mixing ratio	Part A:Part B = 2:1 (by weight)

V. PROCEDURE FOR GROUTING SELF-LEVELING CONCRETE AT THE SITE

Before unloading the reactor, the foundation's top surface was roughened by chipping to enhance mechanical interlock and grout adhesion. The surface was saturated with clean water for 24 h, then brought to a Saturated Surface Dry (SSD) condition by removing free-standing water immediately before self-leveling grout application.

A. Clearance Creation

After the rollers were removed from the reactor tank, a clearance of 150 mm was maintained between the reactor base plate and the RCC foundation block by means of hydraulic jacks.

B. Preventive Sealing Measures

The slot between rail sides and embedded angles was packed with thermocol and sand to prevent grout entry, while oil greased plywood or 22 mm thermocol strips protected rail surfaces from GP2 grout adhesion.

C. Positioning and Leveling

The reactor tank was positioned on pre-arranged shim plates. The level at the reactor curb plate was verified using a 10 mm transparent water level tube. Any discrepancies were corrected by adjusting the shim plates at both ends to achieve uniformity (Figure 8).

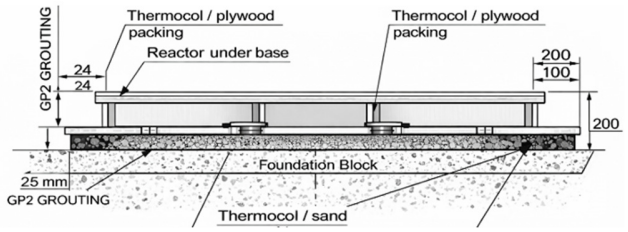

Fig. 8. Reactor mounting setup and shim plate position.

D. Shuttering Installation

Wooden shuttering was installed around the foundation block, projecting 5–10 mm above the reactor base seating plate, to facilitate controlled grout placement and prevent leakage.

E. Grout Preparation

The grout mix, at a 5.5:1 powder-to-water ratio, was blended for 3–5 min using a low-speed high-shear mixer to ensure uniform, timely placement of the grout.

F. Grout Placement

The grout was placed beneath the reactor tank in a single continuous operation to ensure uniform filling and removal of air gaps. It was poured up to shutter height, enabling controlled overflow for complete penetration and void free consolidation.

G. Curing

Post-placement, the grout was allowed to cure under controlled conditions to ensure structural integrity and long-term performance.

H. Pressurized Injection Grouting

Epoxy grout, pressure-injected into cracks, restores structural continuity through superior adhesion, high strength, and effective vibration damping.

I. Surface Leveling

Surface leveling was executed using a high performance, non-shrink leveling compound to reprofile the concrete surface, producing a uniform finish and reducing vibration transmission.

VI. RESULT ANALYSIS

Analytical vibration data showed that although reactor vibrations were within acceptable limits, the foundation exhibited a highly non-uniform dynamic response before retrofitting, with local amplification in cracked and debonded regions.

TABLE VI. BEFORE VS AFTER RETROFITTING – PHYSICAL AND ANALYTICAL COMPARISON

Aspect / parameter	Before retrofitting	After retrofitting
Foundation unevenness/cracks	Multiple cracks; 3–4 mm wide, 500–650 mm deep.	Cracks sealed using self-leveling concrete and pressurized epoxy injection.
Concrete strength	Average equivalent cube strength≈28.64 N/mm².	Damaged zones replaced with micro-concrete, improving stiffness.
Rebar condition	No carbonation; minimal corrosion.	Rebars cleaned, coated with epoxy zinc primer; additional reinforcement.
Vibration – peak-to-peak	Avg=23.25 µm; Max=95 µm (40 points).	≈4.98 (average) ≈23.31 µm(max).
Vibration distribution	12 pts≤10 µm; 15 pts 10–30 µm; 9 pts>30 µm.	Distribution shifted to lower vibration ranges.
Dynamic amplification	Max/Avg≈4.08, indicating local amplification.	≈4.67 Amplification reduced as stiffness restored.
Surface condition	Unevenness, debonding, honeycombing.	Reprofitted using grout; uniform load transfer.
Repair methodology	Loose concrete, open cracks, unprotected steel.	Self-leveling concrete+Epoxy + micro-concrete.

The low maximum-to-average vibration ratio indicated stiffness loss and possible resonance behavior. After retrofitting—particularly through epoxy injection and micro-concrete reconstruction—the foundation is expected to behave monolithically, ensuring uniform force distribution and reduced peak displacements. These improvements enhance operational reliability and minimize future vibration-induced distress. All analyses followed the standards of [5-7]. The results, summarized in Table VI, indicate that, indeed, retrofitting had the expected positive effect on the foundation.

A. Performance Improvement

Post-retrofitting evaluation at 40 points showed a 40–60% reduction in peak-to-peak displacement, with average vibration decreasing from 23.36 µm to 4.98 µm and maximum vibration from 95 µm to 23.31 µm, indicating significantly improved stiffness and dynamic performance. (Figures 9-12).

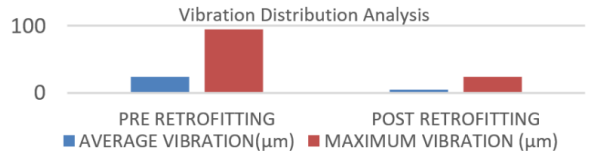

Fig. 9. Vibration distribution pre- and post-retrofitting.

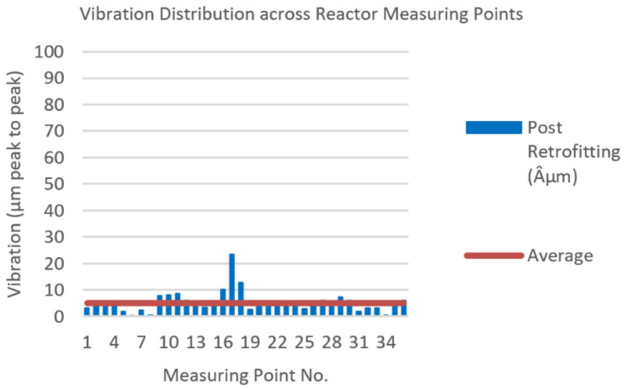

Fig. 10. Maximum and average vibration post-retrofitting.

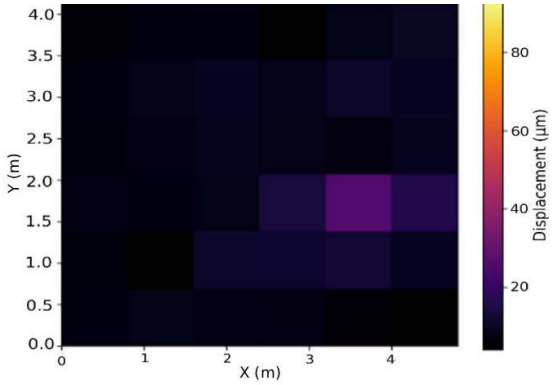

Fig. 11. Heat map post-retrofitting.

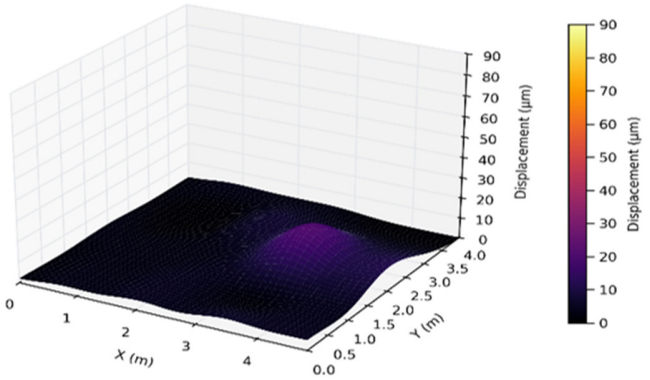

Fig. 12. Three-dimensional view post-retrofitting.

B. Structural Integrity

The disappearance of vibration hotspots near rail anchorage and steel–concrete interfaces confirms restored monolithic behavior, improving load transfer, reducing dynamic amplification, and enhancing long-term reliability, as displayed in the post-retrofitting heat map.

C. Analytical Tools

Python (3.x) was used for numerical analysis, with NumPy utilized for computations, Pandas for data processing, and Matplotlib for visualizing vibration distributions and heat maps, demonstrating effective integration of data-driven methods for structural health monitoring.

VII. CONCLUSION

This study addresses a significant research gap in seismic retrofitting of vibration-sensitive reactor foundations in high-voltage power substations by integrating vibration heat maps analysis with Non-Destructive Testing (NDT) for informed decision-making. Existing literature primarily focuses on conventional repair techniques or isolated diagnostic methods, whereas this work introduces a data-driven approach combining vibration diagnostics and advanced material technologies to enhance structural resilience under dynamic and seismic loads.

The retrofitting strategy included comprehensive surface leveling, crack assessment, precise material selection, and execution under strict safety protocols suitable for a live, charged substation environment. Advanced materials—self-leveling concrete, epoxy injection grout, and micro-concrete—were chosen for their superior flowability, thermal compatibility, and vibration-damping capacity. Post-retrofitting vibration analysis showed improvement, with average displacement decreasing from 23.25 µm to 4.87 µm and peak displacement from 95 µm to 23.31 µm, confirming enhanced structural performance. Regular structural health monitoring is essential for sustaining the reliability of vibration-sensitive substation components. Future reactor foundations should integrate advanced vibration-mitigation features to control displacement and preserve stiffness. Compliance with IS codes and high-quality construction practices is crucial for ensuring long-term structural performance and operational safety.

This study is novel in:

- integrating vibration heat-map diagnostics with NDT for precise identification of stiffness-loss zones.
- introducing a synergistic repair system combining self-spreading concrete, micro-concrete, and pressurized epoxy for vibration-sensitive foundations.
- enabling data-driven, phased retrofitting under live substation conditions.
- demonstrating substantial dynamic improvement with displacement reducing from 23.25 µm to 4.98 µm.

DECLARATION OF COMPETING INTERESTS

There are no competing interests related to the content or publication of this manuscript.

ACKNOWLEDGMENT

The authors confirm that there was no external funding received for conducting this study or preparing the manuscript.

DATA AVAILABILITY

The data supporting the findings of this study will be made available by the authors upon reasonable request.

AI USE AND DECLARATION OF GENERATIVE AI USE

During the preparation of this paper, generative AI tools were utilized exclusively for proofreading, grammar correction, and improving linguistic clarity. No AI-generated content was used for conceptual development or analysis. All ideas and arguments are the original work of the author.

REFERENCES

[1] Q. Fang, Z. Ye, and C. Chen, "A Review of Power Transformer Vibration and Noise Caused by Silicon Steel Magnetostriction," *Electronics*, vol. 13, no. 5, Mar. 2024, https://doi.org/10.3390/electronics13050968.

[2] Y. Feng, T. Wang, D. Wang, J. Wanyan, and C. Wang, "Development of a Novel Vibration Isolation and Damping Device for Power Equipment: Design, Test and Numerical Analysis," *Journal of Earthquake Engineering*, vol. 29, no. 6, pp. 1204–1226, Feb. 2025, https://doi.org/10.1080/13632469.2025.2467306.

[3] C. Kumar, A. K. Sinha, P. Anand, and S. Pandey, "Image Processing Approaches for Identifying Cracks in Concrete Structures," in *Recent Developments in Structural Engineering, Volume 1*, M. D. Goel, R. Kumar, S. S. Gadve, Ed., Singapore: Springer, 2024, pp. 213–221, https://doi.org/10.1007/978-981-99-9625-4_20.

[4] S. K. Dwivedi, M. Vishwakarma, and Prof. A. Soni, "Advances and Researches on Non Destructive Testing: A Review," *Materials Today: Proceedings*, vol. 5, no. 2, Part 1, pp. 3690–3698, 2018, https://doi.org/10.1016/j.matpr.2017.11.620.

[5] *Hardened Concrete – Methods of Test, Part 4 Sampling and Testing of Concrete Cores*, IS516, Bureu of Indian Standards, 2018.

[6] *Products and systems for the protection and repair of concrete structures - Test methods - Determination of carbonation depth in hardened concrete by the phenolphthalein method*, BS 14630:2006, The British Standards Institution, 2006.

[7] *Mechanical vibration - Evaluation of machine vibration by measurements on non-rotating parts,* ISO 10816-3, Second Edition, 2009.

[8] Km. Pooja and N. Tarannum, "Self-healing concrete: a path towards advancement of sustainable infrastructure," *Discover Applied Sciences*,

vol. 7, July 2025, Art. no. 703, https://doi.org/10.1007/s42452-025-06529-w.

[9] A. Bouabdallah, A. Benaissa, M. A. Bouabdallah, S. Malab, and A. Khatir, "Development and performance evaluation of self-leveling sand concrete: Enhanced fluidity, mechanical strength, durability, and non-destructive analysis," *Construction and Building Materials*, vol. 468, Mar. 2025, Art. no. 140463, https://doi.org/10.1016/j.conbuildmat.2025.140463.

[10] K. N. Rajesh, M. K. Rath, and P. M. Raju, "A Research on Sustainable Micro-Concrete," *International Journal of Recent Technology and Engineering*, vol. 8, no. 2S3, pp. 1137–1139, July 2019, https://doi.org/10.35940/ijrte.B1210.0782S319.

[11] W. Wang, W. Zhao, J. Zhang, and J. Zhou, "Epoxy-based grouting materials with super-low viscosities and improved toughness," *Construction and Building Materials*, vol. 267, Jan. 2021, Art. no. 121104, https://doi.org/10.1016/j.conbuildmat.2020.121104.

[12] Z. Chen, Z. Li, Z. Ran, Y. Zhang, F. Lin, and Y. Zhou, "Study on the Performance of Composite-Modified Epoxy Resin Potting Adhesive for Repairing Oblique Cracks," *Materials*, vol. 18, no. 13, July 2025, https://doi.org/10.3390/ma18133197.

[13] N. Akeel, "Testing and Evaluation of the Mechanical Strength of New Epoxy and Silk Composite Materials," *Engineering, Technology & Applied Science Research*, vol. 15, no. 4, pp. 25545–25548, Aug. 2025, https://doi.org/10.48084/etasr.11899.